Cross-correlation of LoTSS DR2 with CMB lensing

Radio galaxy bias and cosmology

Maciej Bilicki
Center for Theoretical Physics PAS, Warsaw, Poland

On behalf of:
Szymon Nakoneczny (Caltech), David Alonso (Oxford)
and the LOFAR Cosmology Team

LOFAR Family Meeting, Olsztyn, 15.06.2023

Disclaimer: work in progress, some results might change before submission

Standard cosmological model: ΛCDM

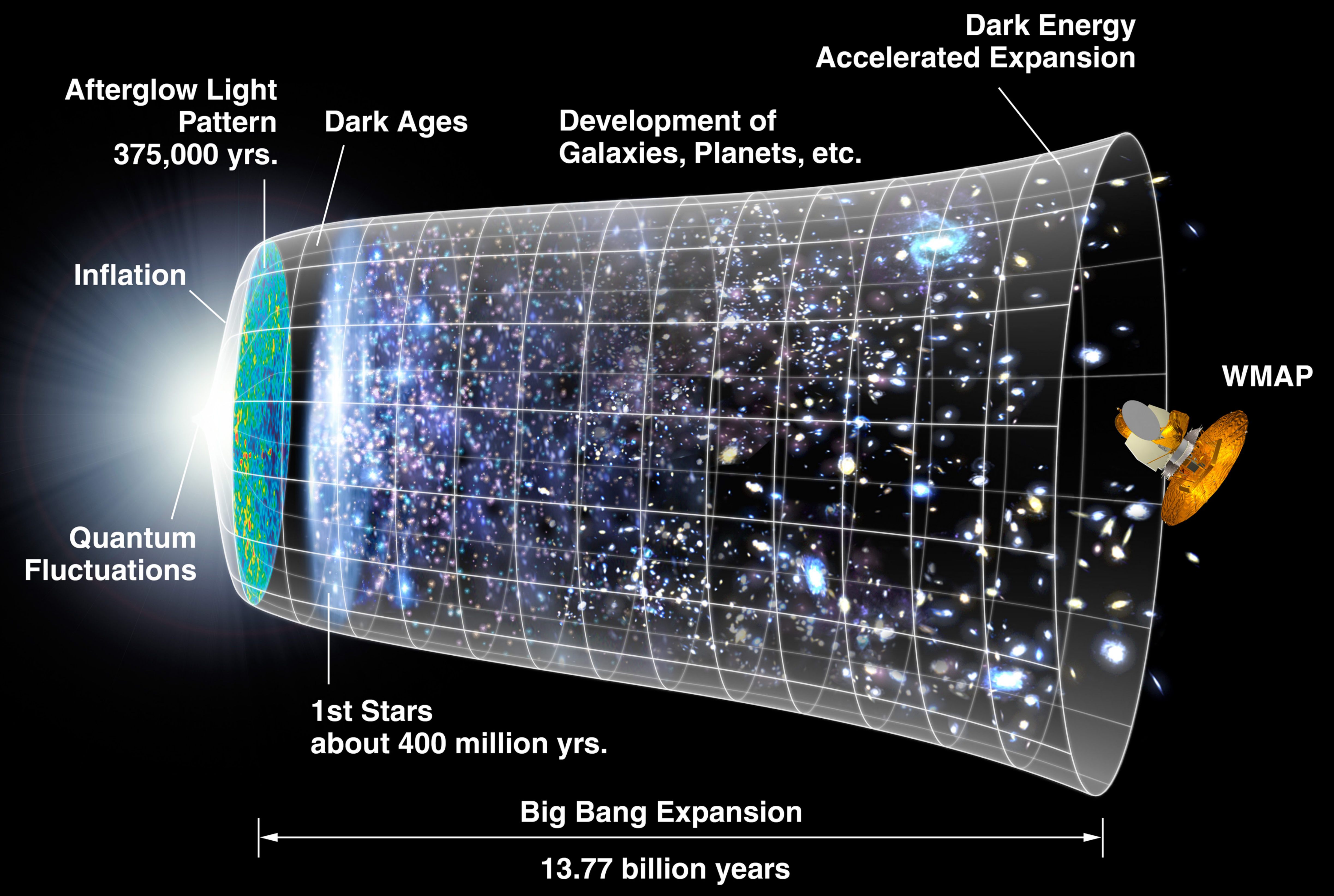

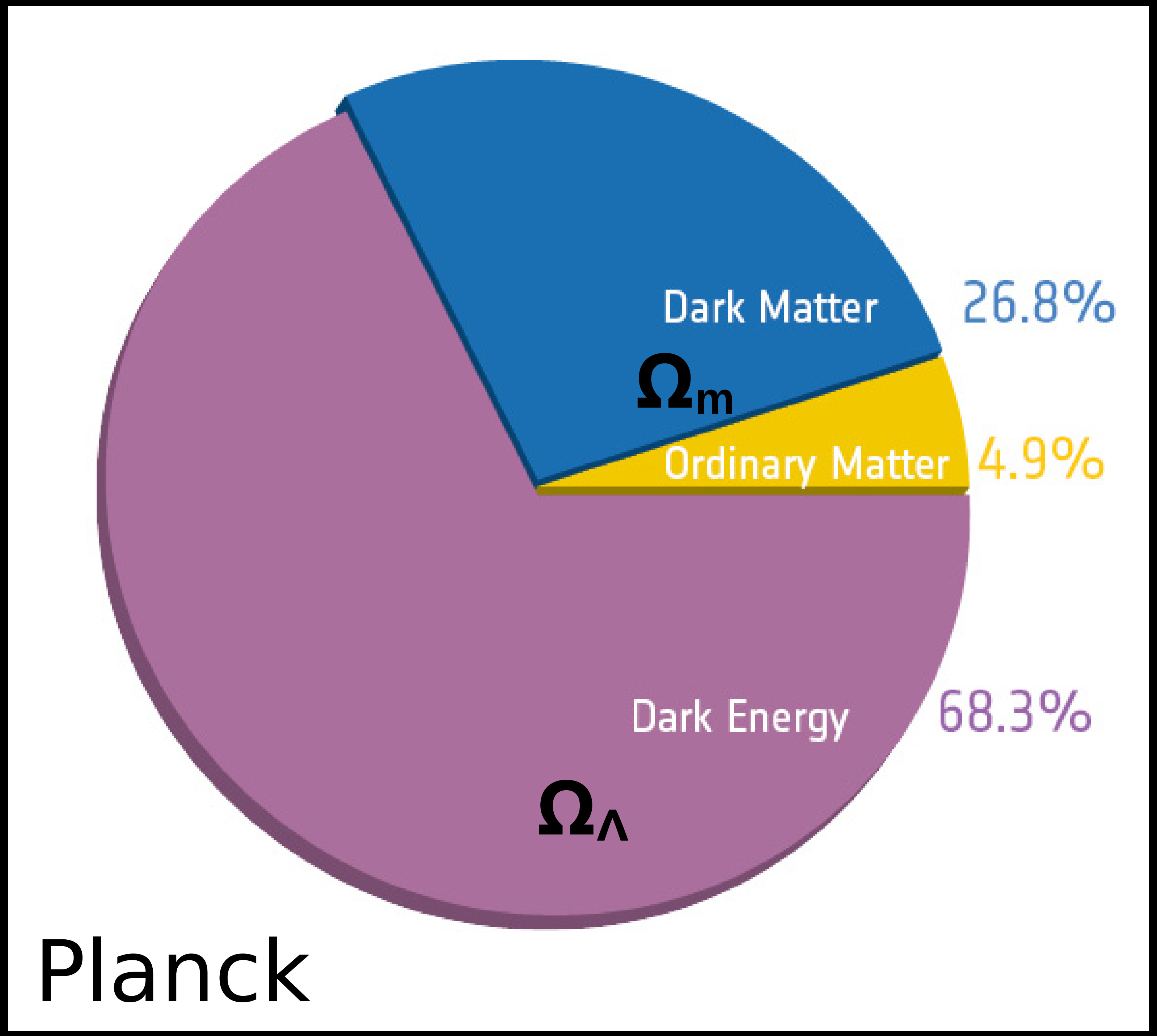

NASA/WMAP Science Team

Cosmological tensions

Hubble constant H_0

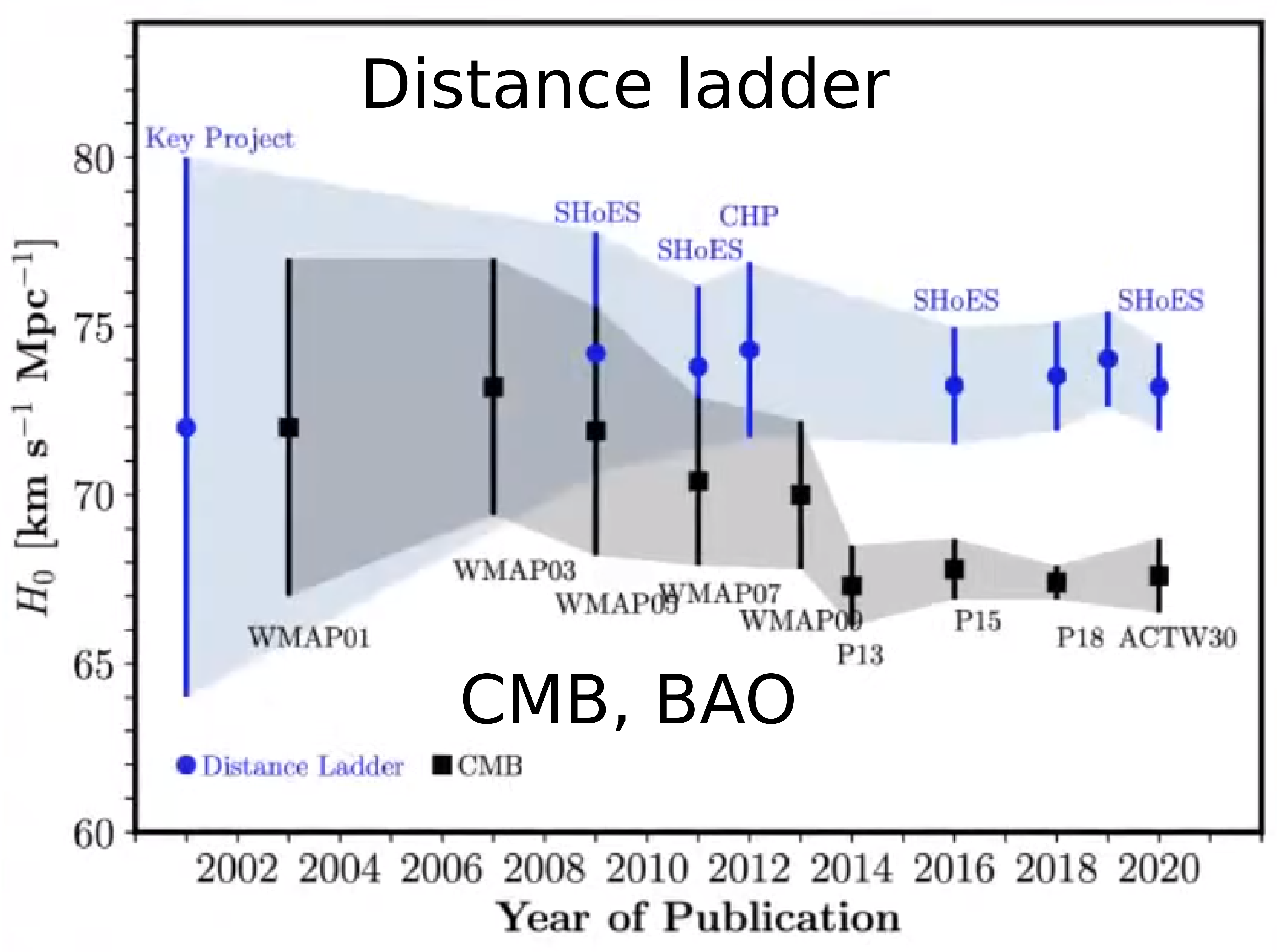

Credit: Wendy Freedman

Current expansion rate

σ_8, S_8

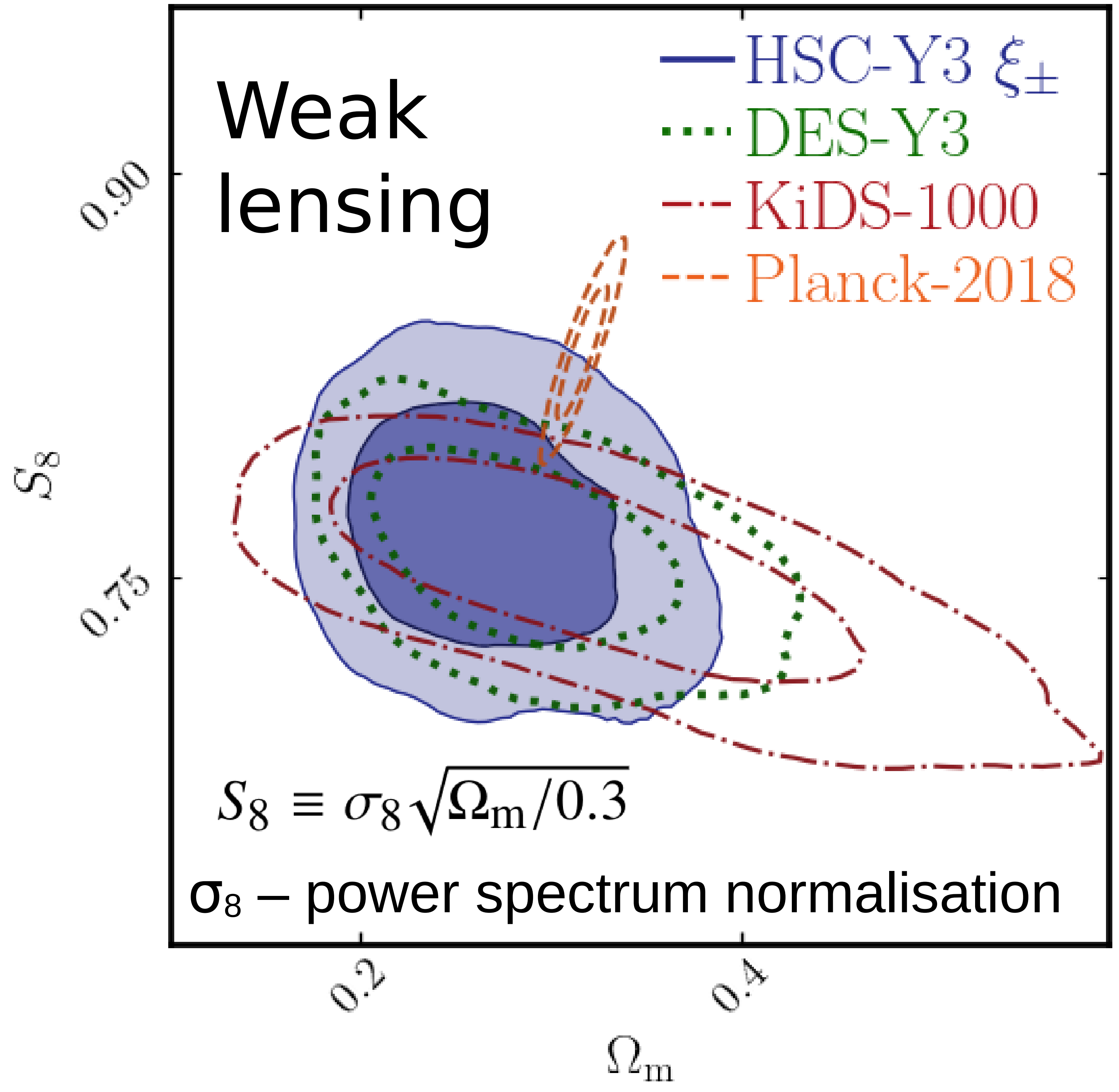

arXiv:2304.00702

Amount of matter fluctuations

Secondary gravitational effects in CMB

Cosmic **M**icrowave **B**ackground interacts with foreground large-scale structure

(i) The integrated Sachs-Wolfe (ISW) effect is due to CMB photons traversing a time-varying linear gravitational potential. The relevant scale is the curvature scale freeze-out in concordance cosmology: the horizon at $1 + z \sim (\Omega_\Lambda/\Omega_\mathrm{m})^{1/3}$. This corresponds to an angular scale of about 10°.

(ii) The Rees-Sciama (RS) effect is due to CMB photons traversing a non-linear gravitational potential, usually associated with gravitational collapse. The relevant scales are those of galaxy clusters and superclusters, corresponding to angular scales of 5-10 arc minutes.

(iii) Gravitational lensing of the CMB by intervening large-scale structure does not change the total power in fluctuations, but power is redistributed preferentially towards smaller scales. The effects are significant only below a few arc minutes. Its effects may be significant on large scales when the observable of interest is the B-mode power spectrum.

Table 1. Sources of temperature fluctuations.

PRIMARY	Gravity	
	Doppler	
	Density fluctuations	
	Damping	
	Defects	Strings
		Textures
SECONDARY	Gravity	Early ISW
		Late ISW
		Rees-Sciama
		Lensing
	Local reionization	Thermal SZ
		Kinematic SZ
	Global reionization	Suppression
		New Doppler
		Vishniac
"TERTIARY"	Extragalactic	Radio point sources
		IR point sources
(foregrounds	Galactic	Dust
&		Free-free
headaches)		Synchrotron
	Local	Solar system
		Atmosphere
		Noise, *etc.*

Max Tegmark (astro-ph/9511148)

CMB lensing

Large-scale structure weakly lenses CMB passing through

Effect quantified by *lensing convergence κ*

$$T(\hat{\mathbf{n}})_{\text{lensed}} = T(\hat{\mathbf{n}} + \mathbf{d}(\hat{\mathbf{n}}))_{\text{unlensed}} \qquad \kappa = \nabla \cdot \mathbf{d}/2$$

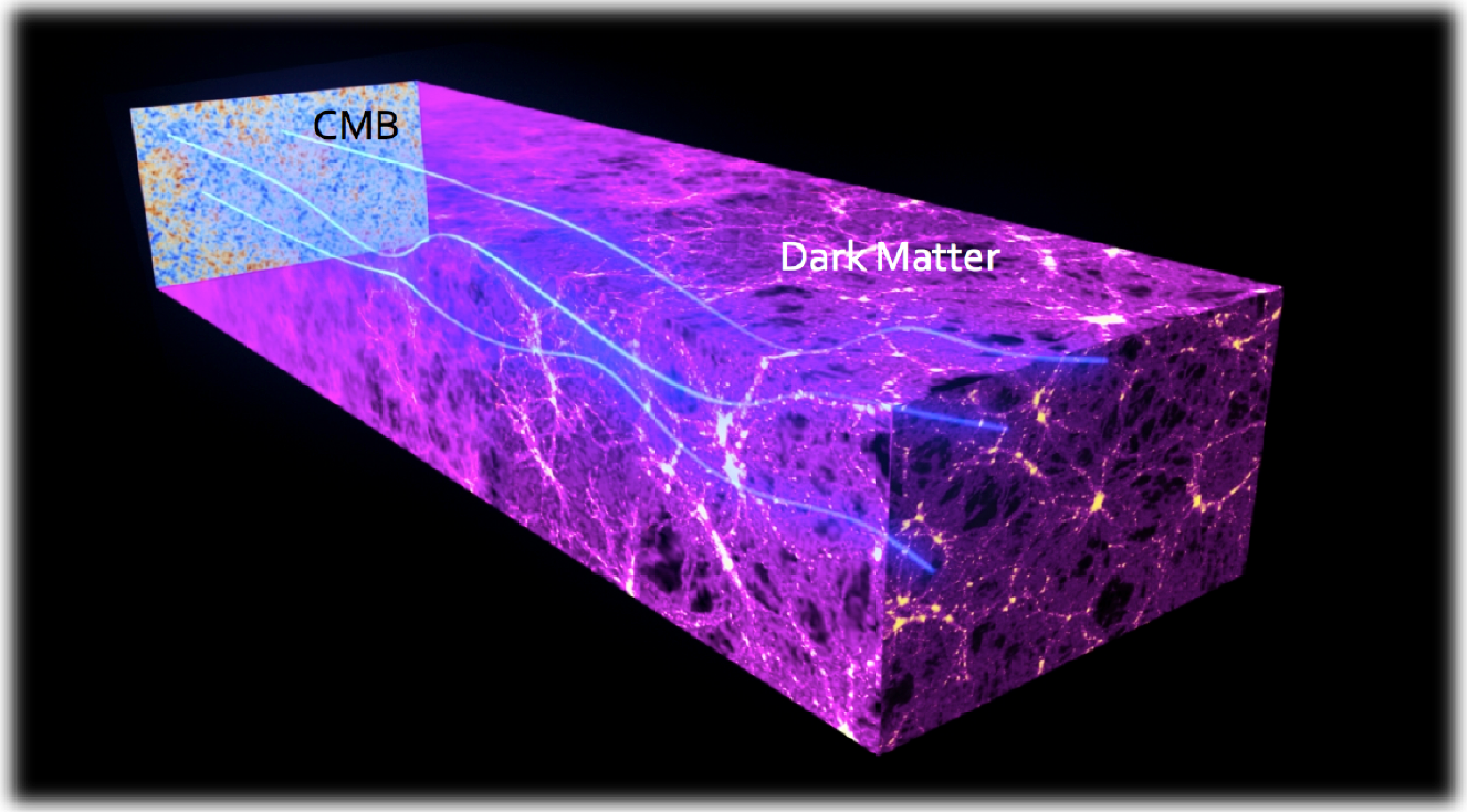

Blake Sherwin, https://kicp-workshops.uchicago.edu/FutureSurveys/depot/materials/sherwin.pdf

CMB lensing

Sky map

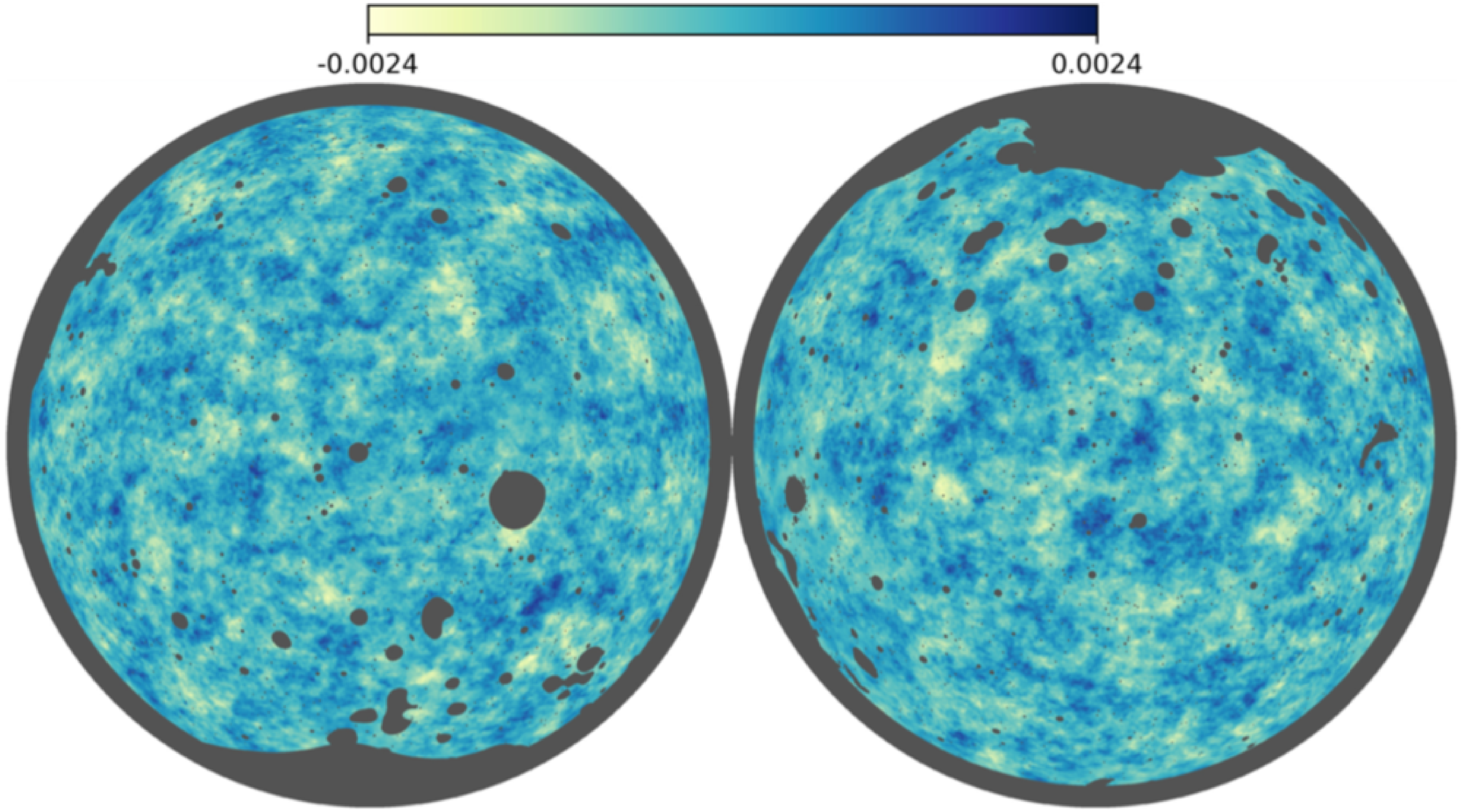

Planck 2018, VIII

Kernel
Compared to LSST galaxies

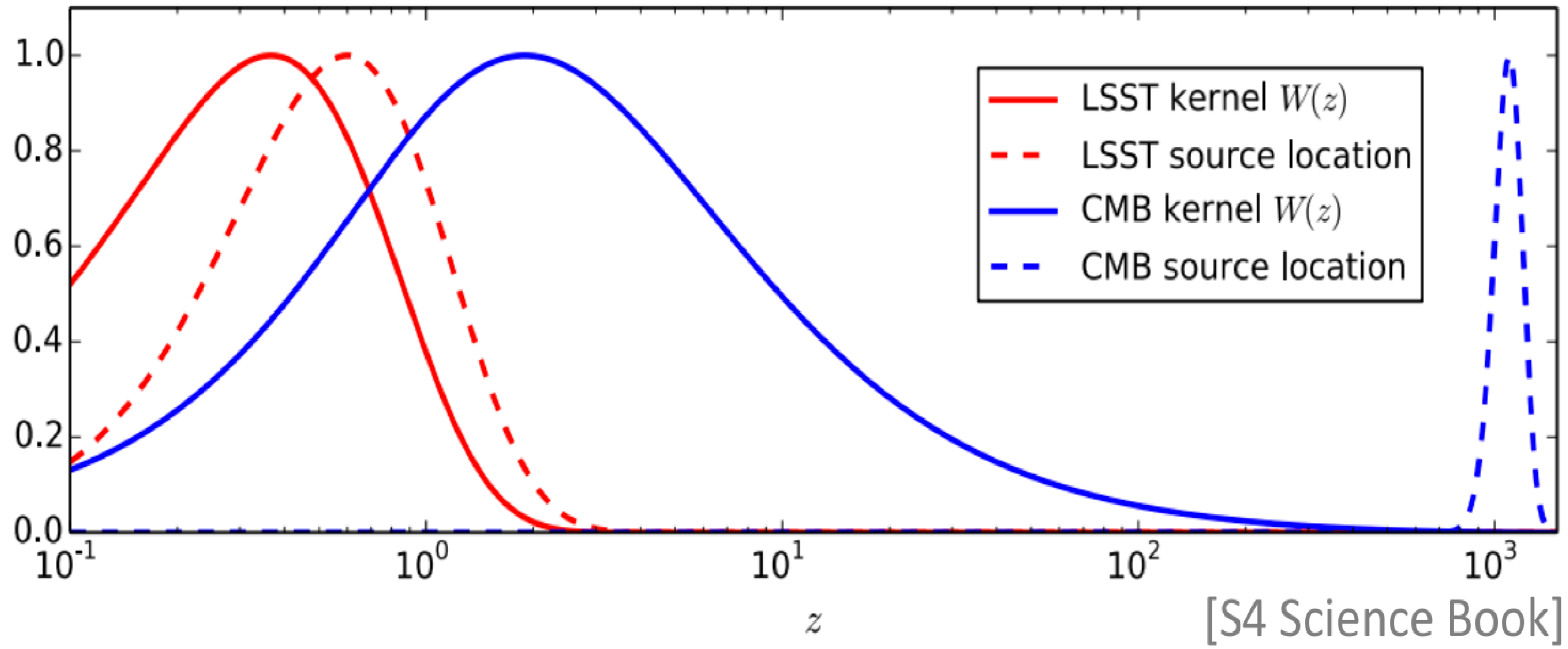

[S4 Science Book]

Integrated effect of the large-scale structure from z~1000 till today

Angular cross-correlation

A method to extract LSS information from CMB

- Galaxy overdensity

$$\delta_g(\hat{\boldsymbol{n}}) \equiv \frac{N_g(\hat{\boldsymbol{n}}) - \bar{N}_g}{\bar{N}_g}$$

$$\delta_g(\hat{\boldsymbol{n}}) = \int \mathrm{d}z \, \frac{\mathrm{d}p}{\mathrm{d}z} \, \Delta_g(\chi(z)\hat{\boldsymbol{n}}, z),$$

$\Delta_g = b \, \Delta_m$

***b* – (linear) galaxy bias parameter**

- CMB lensing convergence

$$\kappa(\hat{\boldsymbol{n}}) = \int_0^{\chi_{\mathrm{LSS}}} \mathrm{d}\chi \, \frac{3H_0^2\Omega_m}{2a} \chi \, \frac{\chi_{\mathrm{LSS}} - \chi}{\chi_{\mathrm{LSS}}} \Delta_m(\chi\hat{\boldsymbol{n}}, z(\chi))$$

- Angular power spectrum

$$C_\ell^{uv} = \int \frac{\mathrm{d}\chi}{\chi^2} W_u(\chi) W_v(\chi) P_{UV}\left(k = \frac{\ell + 1/2}{\chi}, z(\chi)\right)$$

P_{UV} – matter power spectrum, dependent on cosmology (e.g. σ_8)

- Kernels

$$W_g(\chi) = \frac{H(z)}{c} \frac{\mathrm{d}p}{\mathrm{d}z},$$

$$W_\kappa(\chi) = f_\ell \frac{3H_0^2\Omega_m}{2a} \chi \, \frac{\chi_{\mathrm{LSS}} - \chi}{\chi_{\mathrm{LSS}}} \, \Theta(\chi_{\mathrm{LSS}} - \chi)$$

Breaking degeneracies thanks to CMB lensing

LoTSS DR1 (Alonso et al. 2021)

Varying bias

Varying redshift distribution

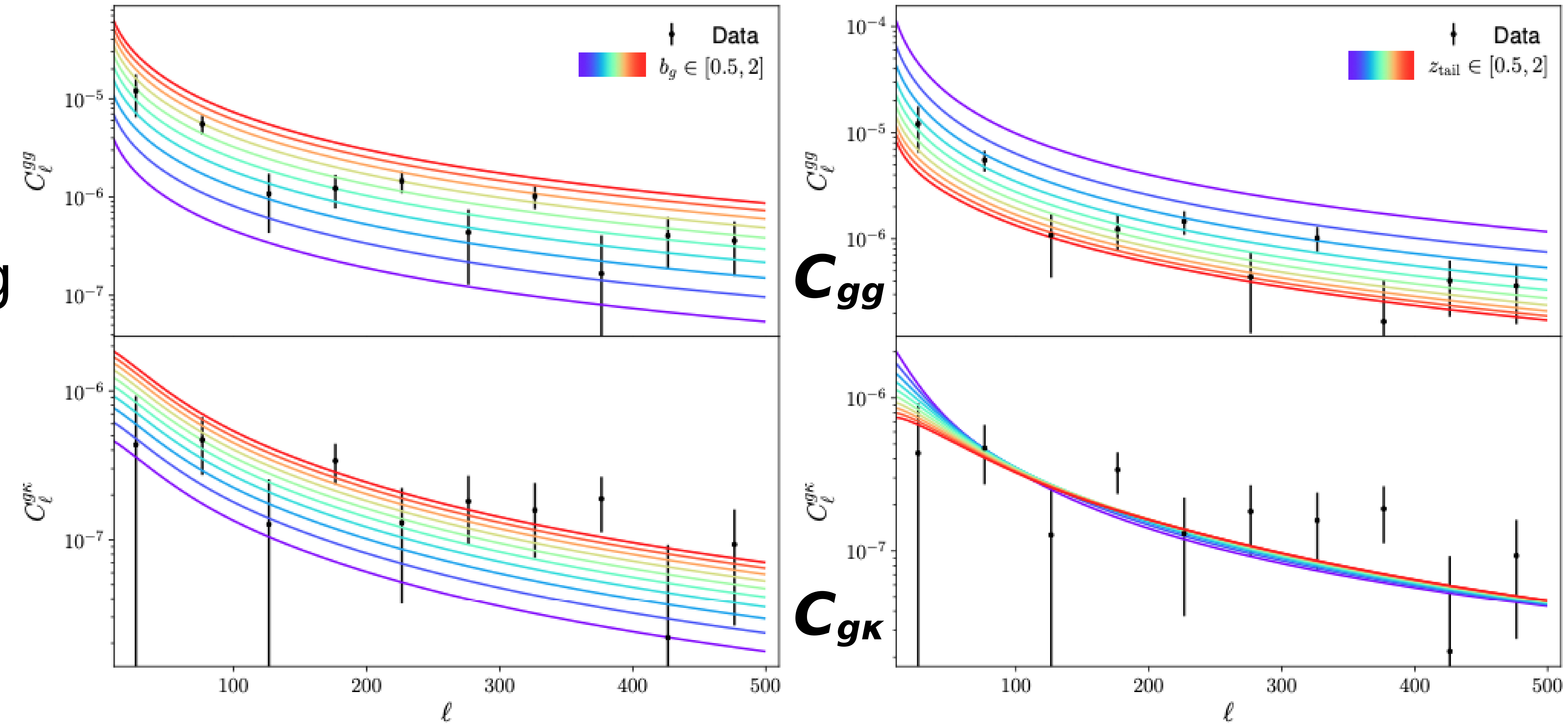

Figure 6. Measured auto- and cross-correlation (black dots with error bars int the top and bottom panels respectively), together with the theory prediction for different values of the galaxy bias b_g and the high redshift tail $z_{\rm tail}$ (left and right panels respectively), both in the range $(0.5, 2.0)$. A "constant amplitude" model is assumed for the redshift evolution of the galaxy bias. b_g is fixed to 1.3 in the right panel, while $z_{\rm tail} = 1.1$ in the left one. While both b_g and $z_{\rm tail}$ affect the amplitude of the auto-correlation, the cross-correlation depends only mildly on the high-redshift tail, making it possible to break the degeneracy between both parameters by combining C_ℓ^{gg} and $C_\ell^{g\kappa}$.

LoTSS DR2

- LOFAR Two-metre Sky Survey (LoTSS) Data Release 2
- 27% of the northern sky
- 4.4 million radio sources before cuts
- **Our selections** (motivated by Hale et al. in prep.):
  → peak flux over 1.5 mJy
  → signal to noise over 7.5
  → fiducial sample of 1.1 million objects

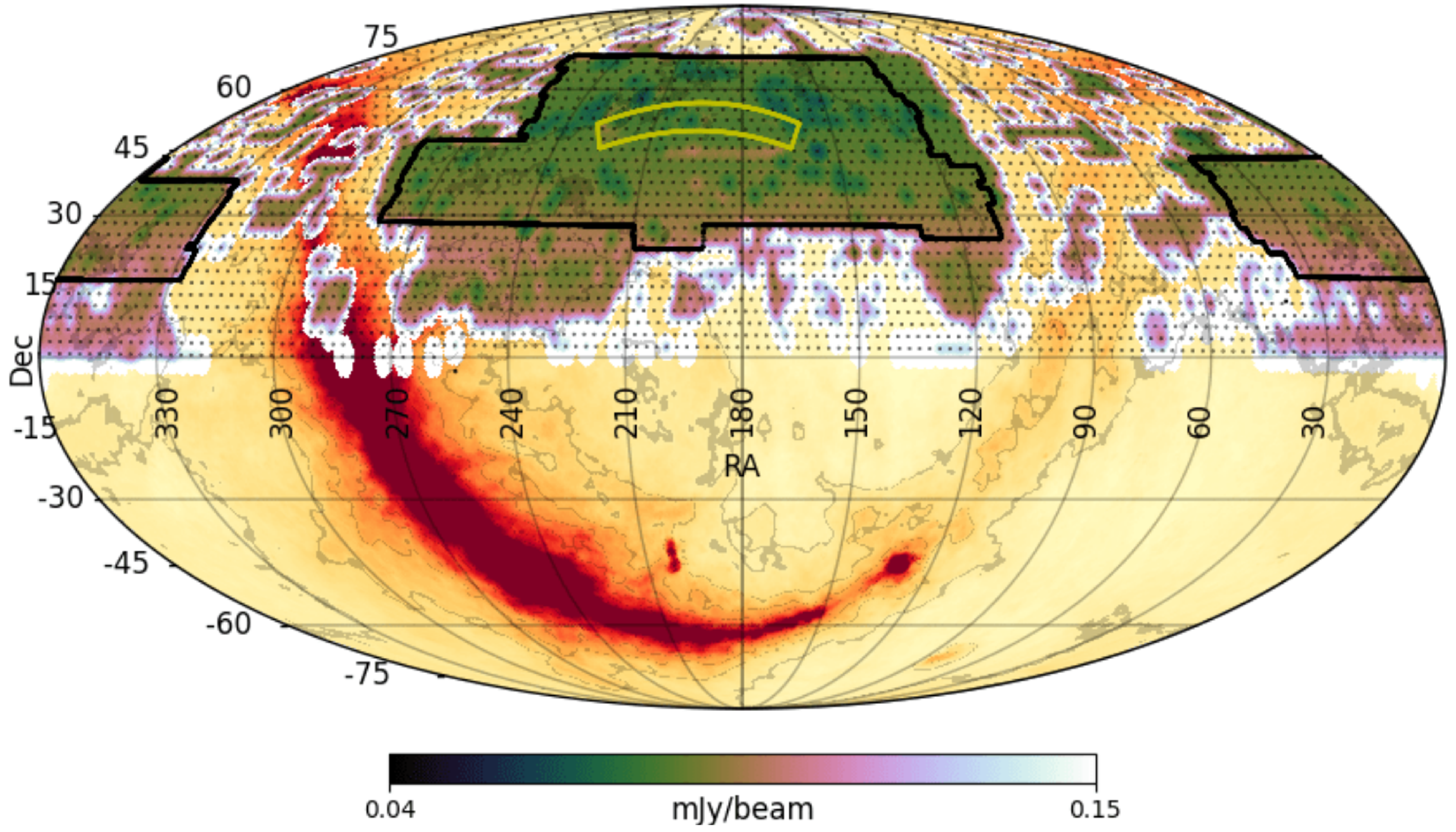

Shimwell et al. 2022

Sky maps

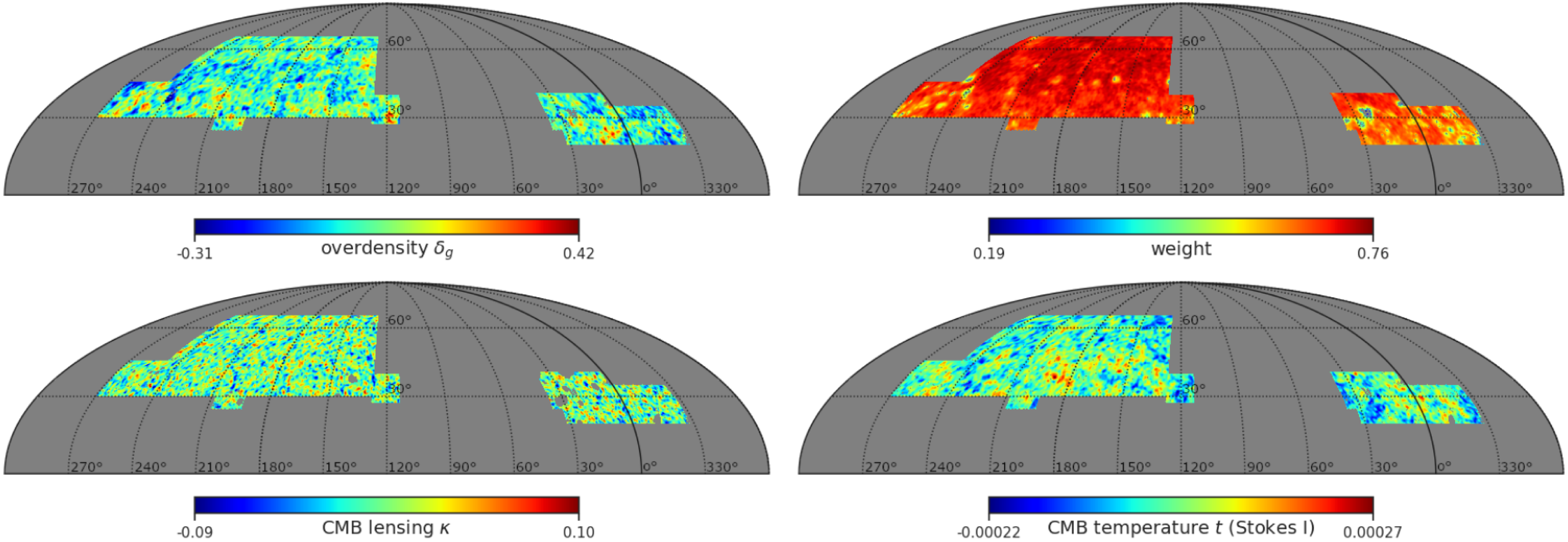

Nakoneczny et al. in prep.

Weights from Hale et al. in prep.

Used to rescale number counts and to generate the mask

Methodology

galaxy autocorrelation
C_{gg}

+

galaxy-CMB lensing
cross-correlation
$C_{g\kappa}$

+

dN/dz
(deep fields)

assuming Planck
cosmology

$\longrightarrow$

linear or Halofit
matter power
spectrum

galaxy bias model

+

redshift distribution model

+

nuisance parameters
(e.g. shot noise amplitude)

[+

additionally σ_8]

Tools

- **NaMaster** (Alonso) – power spectra from observational data (so-called pseudo C_ell, based on Master by Hivon et al. 2002)
- Core Cosmological Library (**CCL**, Chisari, Alonso, Krause et al. 2019) - theoretical modelling of correlations, including Halofit and linear matter power spectrum
- **emcee**, **Cobaya** (Torrado, Lewis 2020) - Monte Carlo Markov Chains and likelihood inference
  - Likelihood

    $$\chi^2 \equiv -2\log p(\boldsymbol{d}|\boldsymbol{q}) = (\boldsymbol{d} - \boldsymbol{t}(\boldsymbol{q}))^T \mathsf{Cov}^{-1}(\boldsymbol{d} - \boldsymbol{t}(\boldsymbol{q})),$$

  - Significance

    $$\mathrm{TS} = \chi^2(0) - \chi^2_{\min} \ ,$$

    sigma = sqrt(TS)

d – data vector including power spectra and redshift distribution

t – theoretical prediction

q – model parameters

LoTSS DR2 redshift distribution

$$\delta_g(\hat{\boldsymbol{n}}) = \int \mathrm{d}z \, \frac{\mathrm{d}p}{\mathrm{d}z} \, \Delta_g(\chi(z)\hat{\boldsymbol{n}}, z), \quad \Delta_g = b \, \Delta_m$$

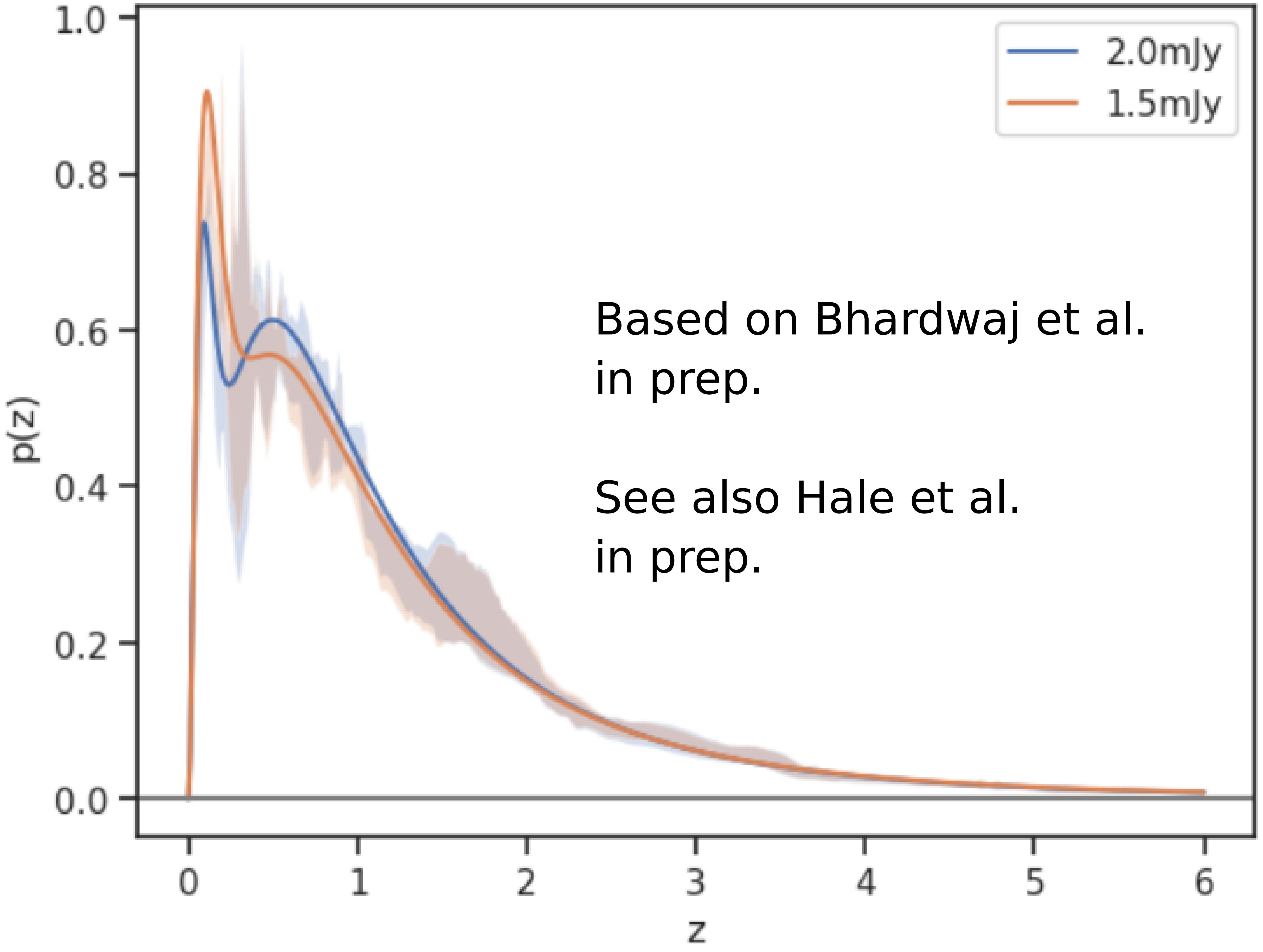

- Shaded: variation from LoTSS Deep Fields (e.g. Duncan et al. 2021)
- Parametrisation:

$$p(z) \propto \frac{z^2}{1+z}\left(\exp\left(\frac{-z}{z_0}\right) + \frac{r^2}{(1+z)^a}\right)$$

models SFGs at low-z and AGNs at high-z

Bias modelling of LoTSS galaxies

$$\delta_g(\hat{\boldsymbol{n}}) = \int \mathrm{d}z \, \frac{\mathrm{d}p}{\mathrm{d}z} \, \Delta_g(\chi(z)\hat{\boldsymbol{n}}, z), \quad \Delta_g = b \, \Delta_m$$

- Three LoTSS DR2 galaxy bias models:

  - Constant (redshift-independent) $\qquad b_g(z) = b_g$

  - "Constant-amplitude" $\qquad b_g(z) = b_{g,D}/D(z)$
    where D(z) is the LSS linear growth factor

  - Quadratic model (empirical) $\qquad b_g(z) = b_0 + b_1 z + b_2 z^2$

- Parameters fitted within MCMC

Correlations

Linear vs. Halofit modelling of matter power spectrum

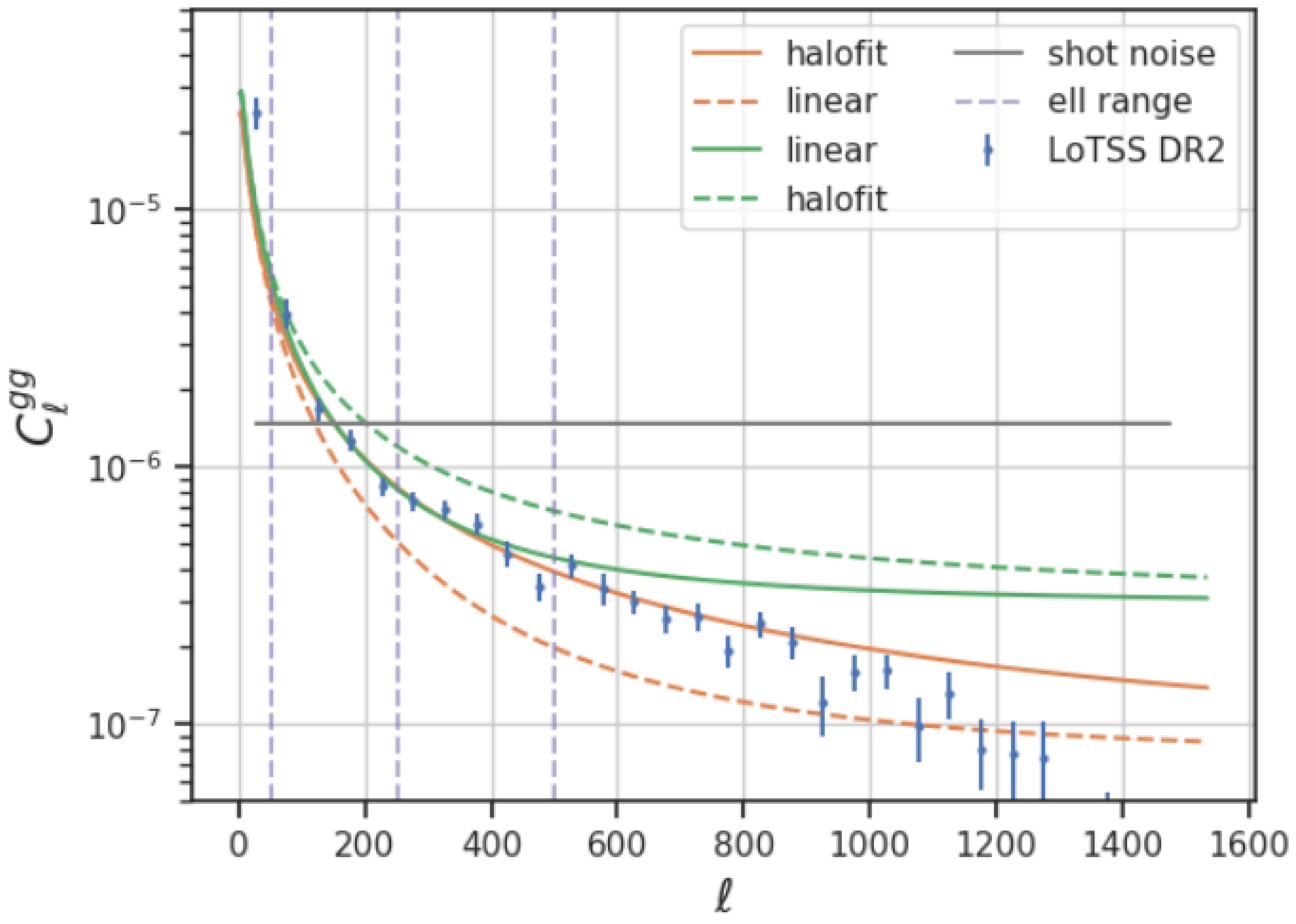

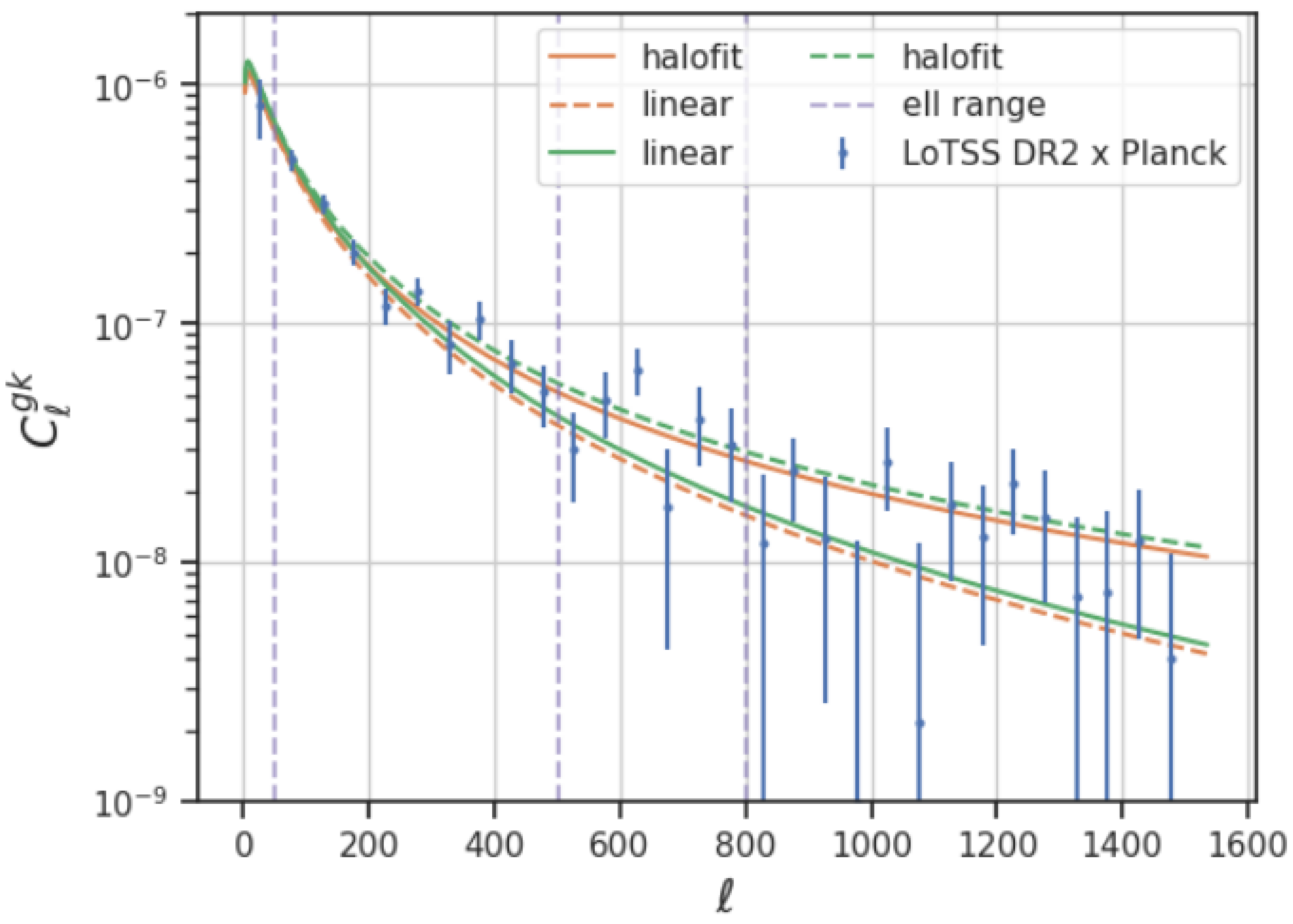

Various multipole ranges tested

Detection at **~23σ** for ell<500
Factor of ~3.6x higher than in LoTSS DR1
(Alonso et al. 2021)

Nakoneczny et al. in prep.

Constraining LoTSS galaxy bias

Constant-amplitude and quadratic models fit the combined C_{gg} & $C_{g\kappa}$ better than constant bias

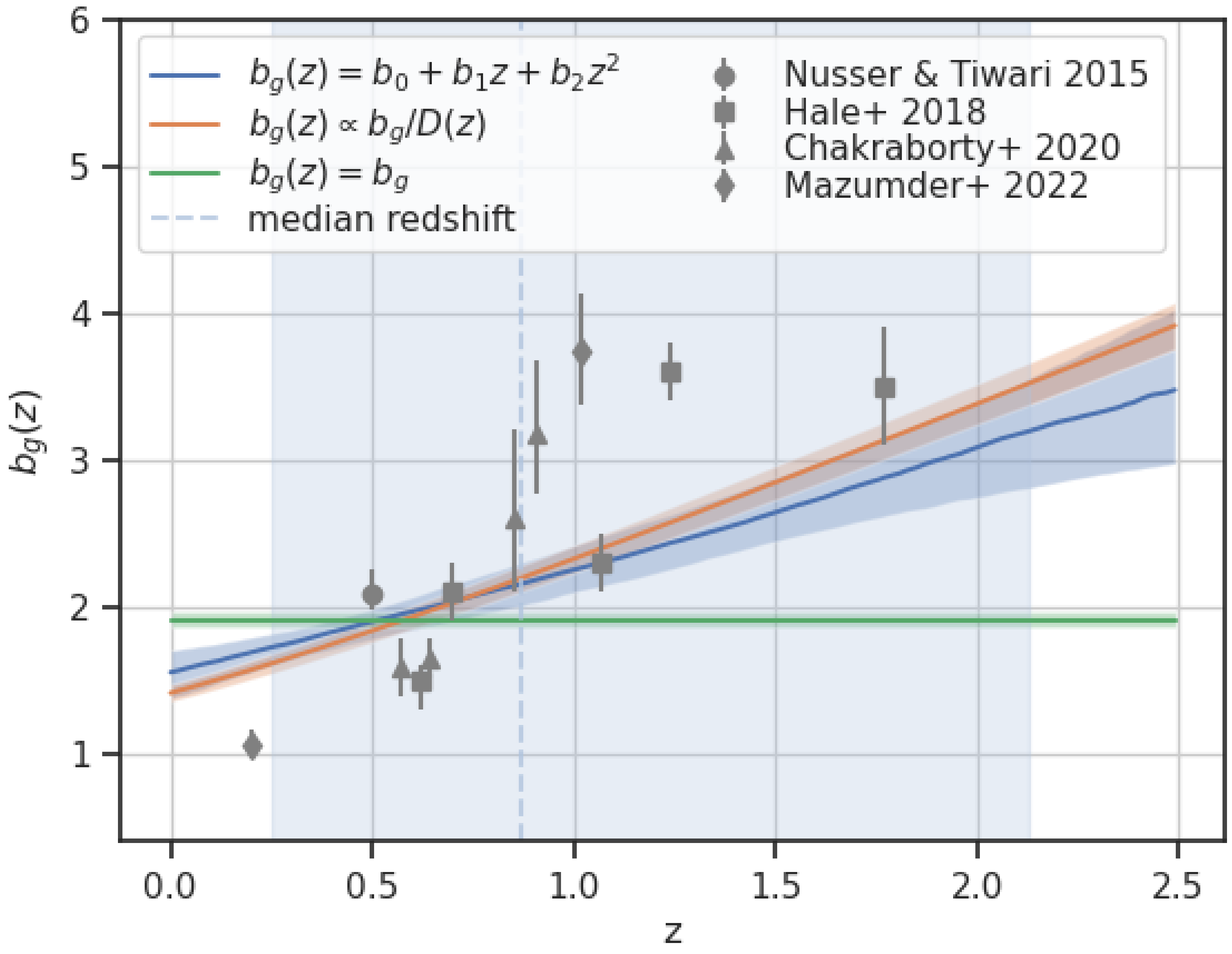

	$b_g(z) = b_g$				$b_g(z) = b_{g,D}/D(z)$			
	b_g	A_{sn}	χ^2	PTE	$b_{g,D}$	A_{sn}	χ^2	PTE
C_ℓ^{gg}	$1.80^{+0.08}_{-0.10}$	$0.98^{+0.09}_{-0.06}$	3.9	41%	$1.49^{+0.06}_{-0.09}$	$0.98^{+0.09}_{-0.05}$	4.0	41%
$C_\ell^{g\kappa}$	$2.17^{+0.09}_{-0.09}$		9.5	39%	$1.39^{+0.06}_{-0.06}$		9.3	41%
C_ℓ^{gg} & $C_\ell^{g\kappa}$	$1.91^{+0.05}_{-0.05}$	$0.93^{+0.04}_{-0.02}$	22.3	5.1%	$1.41^{+0.06}_{-0.06}$	$1.05^{+0.07}_{-0.07}$	14.8	32%

Nakoneczny et al. in prep.

Cosmology constrains

Currently varying only σ_8, other parameters fixed to Planck

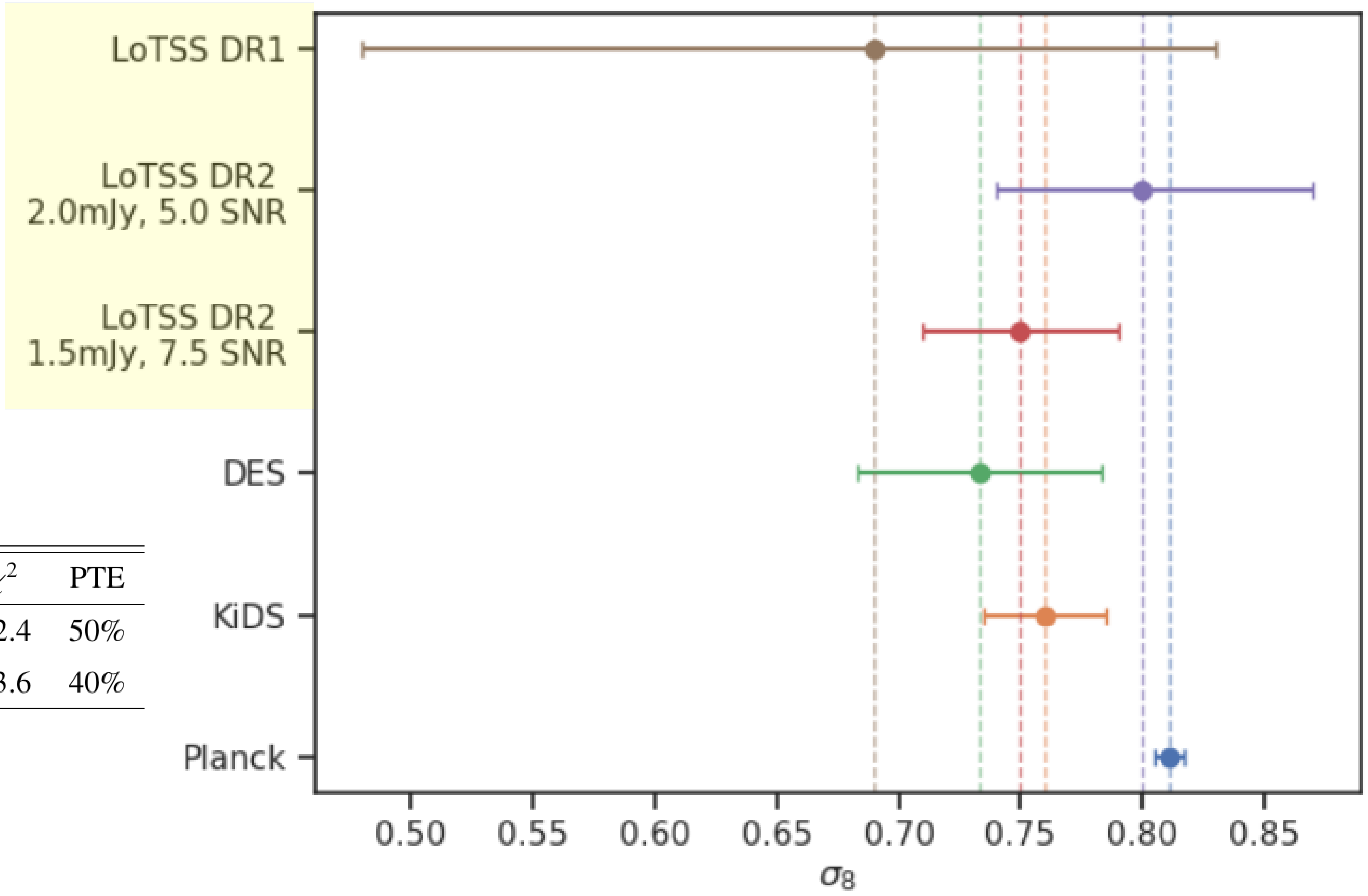

Best fit for
flux>1.5 mJy & SNR>7.5:

$$\sigma_8 = 0.75 \pm 0.04$$

Sample	σ_8	$b_{g,D}$	A_{sn}	χ^2	PTE
(1.5 mJy, SNR > 7.5)	$0.75^{+0.04}_{-0.04}$	$1.64^{+0.16}_{-0.17}$	$0.98^{+0.09}_{-0.08}$	12.4	50%
(2 mJy, SNR > 5)	$0.80^{+0.07}_{-0.06}$	$1.42^{+0.21}_{-0.21}$	$1.18^{+0.09}_{-0.09}$	13.6	40%

Nakoneczny et al. in prep.

Conclusions

- High-significance detection of LoTSS DR2 x CMB lensing cross-correlation
- Bias model constraints, constant model not a good fit
- Underlying redshift distribution is an important ingredient
- Derived σ_8 currently agrees with both Planck and cosmic shear surveys
- Final results with full-sky LoTSS should provide an important test of state-of-the-art cosmological constraints